IMPROVING M_s ESTIMATES BY CALIBRATING VARIABLE PERIOD MAGNITUDE SCALES AT REGIONAL DISTANCES

Heather Hooper[1], Ileana M. Tibuleac[1], Michael Pasyanos[2], and Jessie L. Bonner[1]

Weston Geophysical Corporation[1] and Lawrence Livermore National Laboratory[2]

Sponsored by National Nuclear Security Administration
Office of Nonproliferation Research and Engineering
Office of Defense Nuclear Nonproliferation

Contract Nos. DE-AC52-04NA25547[1] and W-7405-ENG-48[2]

ABSTRACT

One of the most robust methods for discriminating between explosions and earthquakes is the relative difference between the body-wave (m_b) and surface-wave (M_s) magnitudes for a seismic event. Most M_s formulas have been developed for teleseismic distances and for Rayleigh waves in the period range of 17-23 seconds. For small-to-intermediate yield explosions recorded at regional distances, the amplitudes for Rayleigh waves in this period range may be below background noise levels; however, shorter period surface waves (< 15 sec) may still be extracted and processed using phase match filtering. Thus, calibrated and transportable formulas, which allow for estimation of M_s at regional distances at the period of maximum amplitude (between 8 to 25 seconds) are required to lower the M_s thresholds for small earthquakes and explosions. Additionally, these calibrated formulas may be able to significantly reduce the variance in M_s estimates for larger events in the region.

For small events, detection of a Rayleigh wave is often difficult to achieve; thus we are attempting to develop an automated method for surface wave detection and magnitude estimation. First, Rayleigh phases are identified using a detector modeled after the Chael (1997) automatic teleseismic Rayleigh-wave detection method; however, we have modified the detector for regional distance and for 8-25 sec period applications. The modifications include: 1) application of six zero-phase Butterworth filters centered on periods of 9, 12, 15, 20, 22 and 25 seconds; 2) calculation of the covariance matrix for rotated waveforms; and 3) addition of three new weights of the detection function; two for planarity and one for group velocity verification. We have tested the detector on United States Geological Survey (USGS)-located events from eastern and southern Asia. Second, variable-period magnitude formulas are applied, including the new M_s (VMAX) technique (Bonner et al., 2005), on surface waves extracted by automated phase-match filtering. Information for phase match filtering is provided by updated regional tomographic group velocity models of Eurasia, which we are attempting to extend to periods of 10 seconds or less in southern Asia.

OBJECTIVES

Developing a methodology for calculating surface wave magnitudes that is valid at both regional and teleseismic distances, applicable to events of variable sizes and signal-to-noise ratios (SNR), calibrated for variable structure and propagation, and easy to automate in an operational setting is an important monitoring goal. Our objectives are to create such a methodology, and to use it to lower M_s estimation and detection thresholds. We hope that the method will provide a seamless tie between M_s estimation at regional and teleseismic distances.

Our methodology includes the following:

- Extending the geographic coverage of existing group velocity tomography maps to our entire study area, as well as extending the maps to periods of 10 seconds or less,
- Using a semi-automated Rayleigh wave detector to verify that the waveforms contain fundamental-mode Rayleigh waves,
- Using the updated group velocity maps and automated phase match filtering to extract the surface waves from the waveforms,
- Using a variable-period maximum amplitude M_s formula based on Russell (2005) to calculate M_s,
- Calibrating that formula and others for regional distance applications at a number of stations in the study area, and
- Developing empirical and theoretical M_s threshold maps of the study area.

We are in the first stages of this project, which includes updating our group velocity models for Eurasia, developing the Rayleigh detector, developing a phase match filtering routine, and performing preliminary calculations of M_s.

RESEARCH ACCOMPLISHED

Updates to Group Velocity Models

Global and regional group velocity models serve an important function for nuclear monitoring efforts using surface wave analysis. The models serve as input into automated processing routines that can extract small amplitude surface-wave arrivals (e.g., Herrin and Goforth, 1977; Stevens and McLaughlin, 2001), thus lowering M_s detection thresholds. Recent efforts in developing these models have focused on the shorter periods (Levshin et al., 2002; Pasyanos et al., 2003; Taylor et al., 2003).

One region of nuclear monitoring interest which is poorly constrained in current group-velocity tomographic maps is southern Asia. The current coverage is mainly composed of dispersion data from the GEOSCOPE station HYB in Hyderabad, India, along with a few recordings from stations at PUNE (western India), PALK, and a few other open data sources. However, the geometry of the sources and limited stations is such that there are relatively few crossing paths, which are needed to improve the resolution of the models.

Using data collected in southern Asia, we have increased our understanding of the group velocity structure in this region. This has included incorporating the data and results from Mitra et al. (in review) into our models. Mitra et al. used one-dimensional path-averaged dispersion measurements for 1001 source-receiver paths to produce tomographic images between periods of 15 and 45s (Figure 1). Testing of the group velocity models demonstrates that the average resolution across the region ranges from 5 to 7.5 degrees for the periods used in this study.

We are also working to extend our group velocity models of Eurasia to lower periods. Using short period data from stations in India, we are completing new tomographic inversions in order to extend the models to periods of 10 seconds or less. These short-period observations are needed to improve the automated phase match filtering of surface waves.

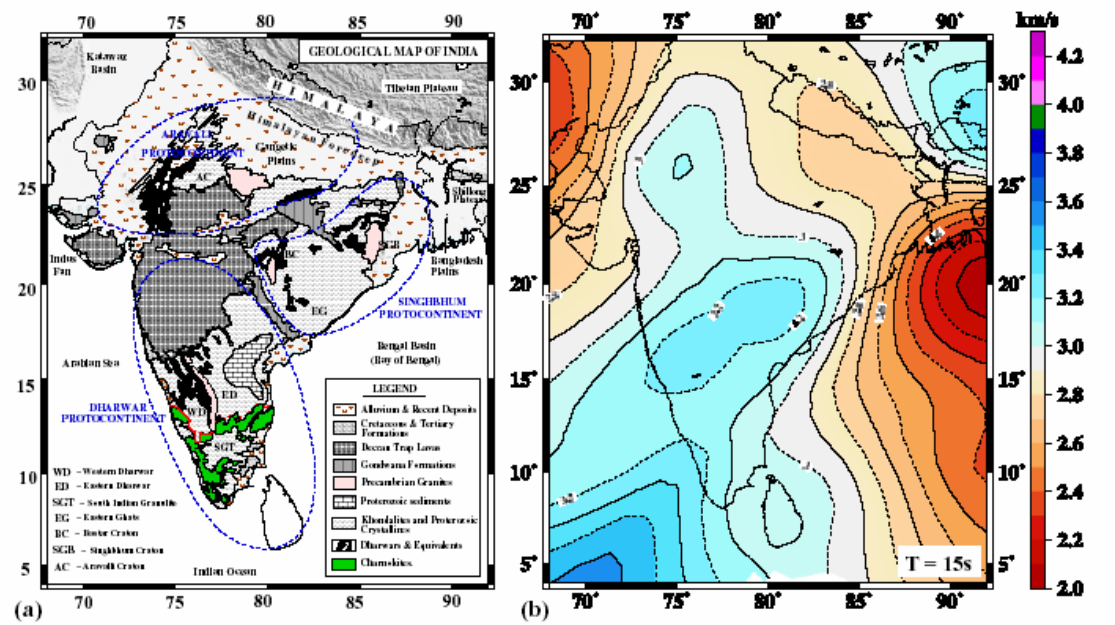

Figure 1. A comparative plot of (a) the geology and tectonics of southern Asia and (b) the tomographic group velocity at a period of 15 seconds, after the work of Mitra et al. (in review). These data have been incorporated into our models of southern Asia and Eurasia.

Semi-Automatic Rayleigh Wave Detection Method

To estimate variable-period (8 to 25 second) regional surface-wave magnitudes, we must first identify Rayleigh-wave phases. We use a semi-automatic detector, similar to an *Rg* detection algorithm developed by Tibuleac *et al.* (2004) and modeled after the Chael (1997) automatic teleseismic Rayleigh-wave detection method. We have modified the detector for regional distance and for 8-25 second period applications. The modifications include: 1) Application of six zero phase Butterworth narrow band filters centered on periods of 9, 12, 15, 20, 22 and 25 seconds. One of these periods is chosen by the analyst to estimate the back azimuth; 2) Calculation of the covariance matrix for rotated waveforms; and 3) Addition of three new weights of the detection function: two for planarity and one for group velocity verification. We have observed that selection of an appropriate frequency band is essential for back azimuth accuracy and for regional Rayleigh wave identification.

We have tested the detector on 154 USGS-located events (Figure 2) with a magnitude range of $3 < m_b < 5.2$, recorded between Jan. 2000 and Dec. 2001 at the WMQ (Urumqi, Xinjiang, China) seismic station, located at 43.8211 N, 87.695 E. Out of 154 analyzed events, an analyst identified 140 Rayleigh phases (91%). For an acceptable back azimuth error of 45 degrees, 121 (86% of the analyst-accepted events) were detected automatically. Three events (2%) were false alarms. 19 events (14%) were automatically rejected. Figure 3 shows the detector performance. The mean Rayleigh back azimuth residual (Figure 3, left plot) was -3.5 degrees, with a sample standard deviation of 15.7 degrees. Most of the Rayleigh phases that were not detected automatically but were confirmed by the analyst (open circles in Figure 3), show back azimuth residuals between 45 and 90 degrees, and are located 400 to 500 km from the station. Analyst-detected Rayleigh arrivals with an estimated detection angle up to 90 degrees off the great circle path are observed when Love waves overlap the Rayleigh waves (Figure 4, upper plots). For this reason our acceptable automatic back azimuth error (45 degrees) was larger than in other studies (Selby, 2001). The semi-automatic routine we have developed can detect Rayleigh phases from events with body-wave magnitude larger than 3, arriving from distances between 250 and at least 1500 km. Further work is needed to address the Rayleigh-Love phase interference as well as integration of multiple filtering in an entirely automatic algorithm. Figures 4 and 5 show an example of the detector output for an m_b=4.5 earthquake that occurred on March 17, 2000, 01:20:39.6, 844.3 km from WMQ, at 40.82 N, 78.24 E, with a depth of 51.8 km, and a back azimuth of 250 degrees.

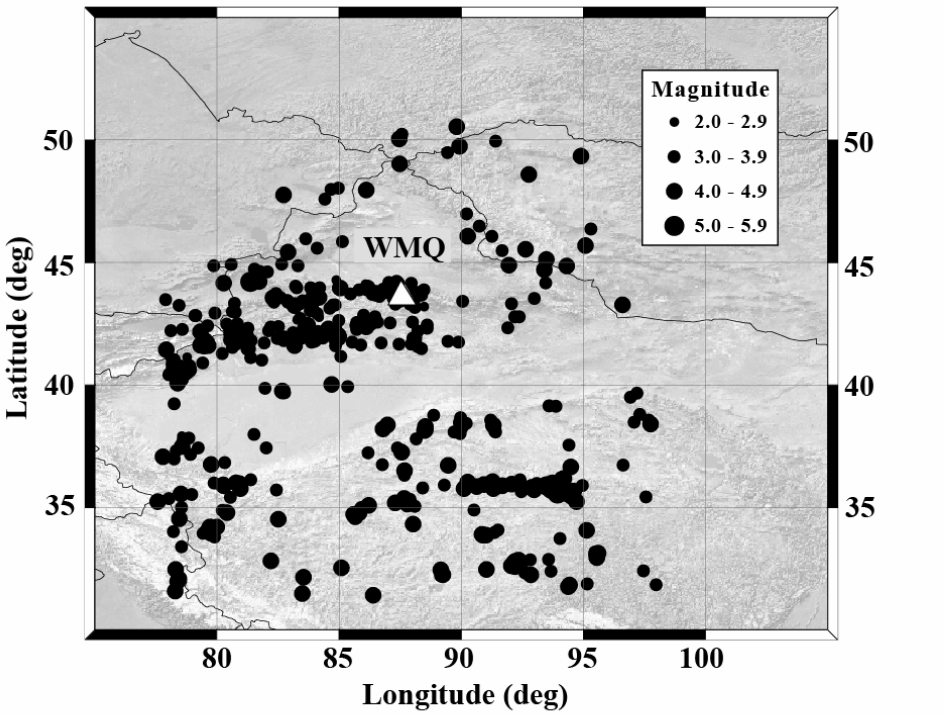

Figure 2. Locations of the events and of the WMQ seismic station.

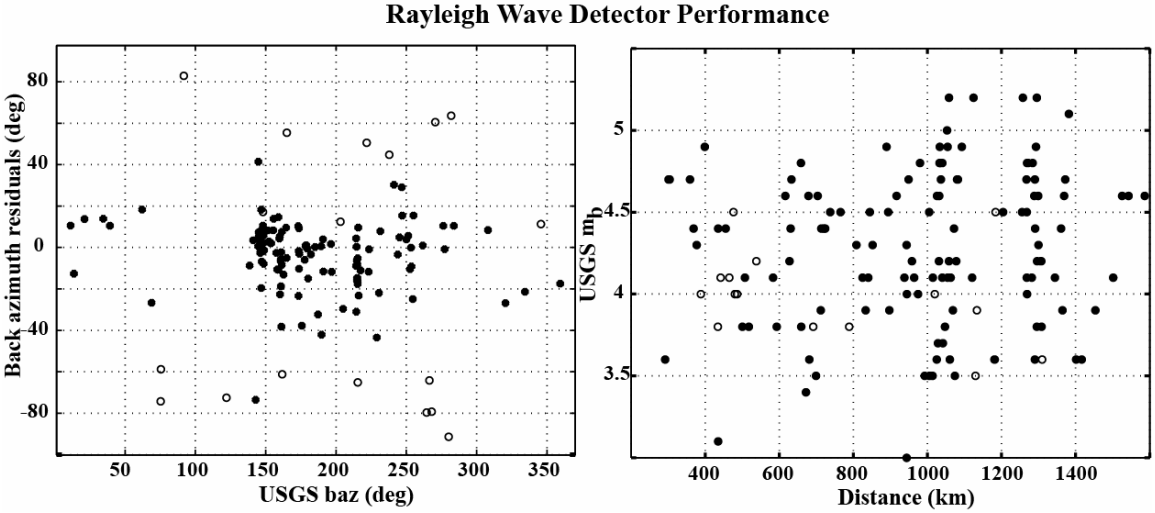

Figure 3. (Left) Back azimuth residuals as a function of USGS back azimuth. The residuals are calculated as the difference between detector-estimated and USGS-estimated back azimuth. Dots represent automatic detections, while open circles represent analyst detections that were rejected automatically. (Right) Detector performance as a function of event epicentral distance and USGS body-wave magnitude. Symbols are the same as in the left plot.

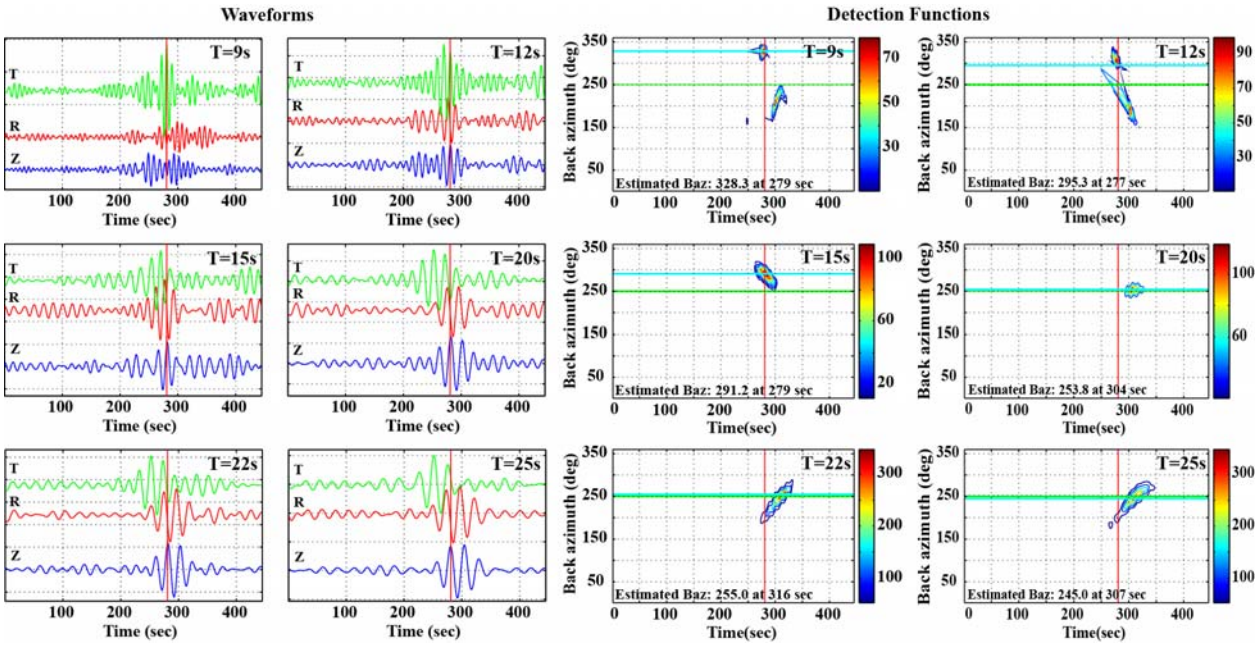

Figure 4. Example of detector output for an m_b=4.5 earthquake that occurred on March 17, 2000, 01:20:39.6, 846.6 km from WMQ, at 40.82 N, 78.24 E, with a depth of 51.8 km, and a back azimuth of 250 degrees. (Left) Waveforms rotated to the USGS-estimated back azimuth and filtered using six zero-phase Butterworth filters centered on periods of 9, 12, 15, 20, 22 and 25 seconds. Rayleigh phases arrive at a time lag of approximately 250 seconds. (Right) Detection function values as a function of time and back azimuth for the filtered waveforms shown at left. The green line represents the USGS-estimated back azimuth, and the cyan line represents the detector-estimated back azimuth. The detector-estimated back azimuths vary from the USGS values by up to 50 degrees for filters centered on 9, 12 and 15 second periods. This effect is caused by the simultaneous arrival of large-amplitude Love phases with the Rayleigh phases at those periods. The vertical red lines represent a group velocity of 3km/s.

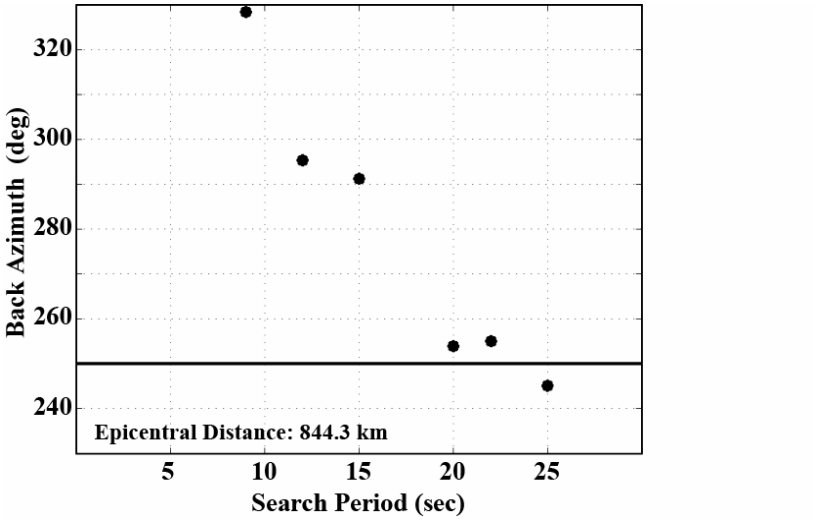

Figure 5. An example of detector-estimated back azimuth variation as a function of the filter center period for the event shown in Figure 4. The black line represents the back azimuth to the USGS location (250.07 degrees). Better back azimuth estimates are achieved when the Rayleigh waves do not overlap the Love wave train.

Phase Match Filtering

We use phase match filtering (PMF) (Herrin and Goforth, 1977; Herrmann, 2004) to extract the surface waves from the seismograms. We use the group velocity dispersion curves obtained from the group velocity tomographic maps (discussed above) for each event-station path to find and apply a filter that has approximately the same phase as the Rayleigh wave signal of interest. This technique improves the signal-to-noise ratio for the extracted surface waves by compressing the dispersed surface-wave signals and removing the effects of microseismic noise, multipathing, body waves, higher-order surface waves, and coda (Pasyanos et al., 1999). Figure 6 shows an example of phase match filtering for the m_b=4.5 sample event shown in Figures 4 and 5.

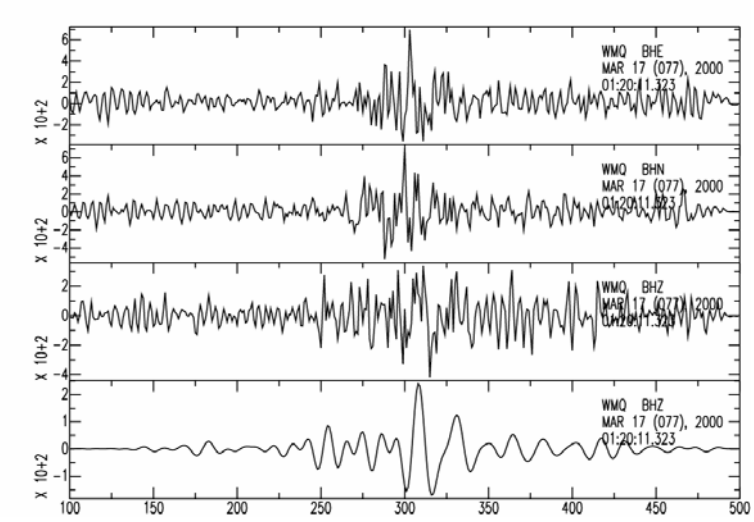

Figure 6. Three-component data from the sample event shown in Figures 4 and 5. The top three panels show the east, north and vertical components of the data. The bottom panel shows the vertical component after phase match filtering. The Rayleigh wave begins at approximately 250 seconds.

M_s Estimation

At regional distances, surface-wave trains are not well dispersed and are often characterized by a pulse-like shape with dominant periods ranging from 5 to 12 seconds. Thus, it is difficult, and for small events often impossible, to determine an M_s as it was originally defined for 17 to 23 second Rayleigh waves. An M_s scale that can incorporate variable periods is required to examine the performance of the M_s-m_b discriminant for small events recorded at regional distances. The maximum amplitude variable-period methodology that we are developing, which includes an M_s formula based on Russell (2005), will reduce the variance at large magnitudes and increase the detection and applicability thresholds, as well as avoid problems associated with depth as long as the event is within the crust or upper mantle.

After phase match filtering has extracted the surface waves of interest, the next step is to measure the amplitudes of the Rayleigh waves in the various frequency bands. The choice of the filtering method is very important to our goal of reducing the variance in the M_s estimates. Building on the work of Yacoub (1983) and Russell (2005), we use a "comb" method in which 18 Butterworth narrow band-pass filters are applied at center periods of 8 to 25 seconds. The filters are applied to the autocorrelation function output of the phase match filtering method, thus helping to remove the effects of Airy phases and dispersion. Figure 7 shows an example of these "comb" filters applied on the previously discussed sample event for both phase match filtered (right) and non-phase match filtered (left) data.

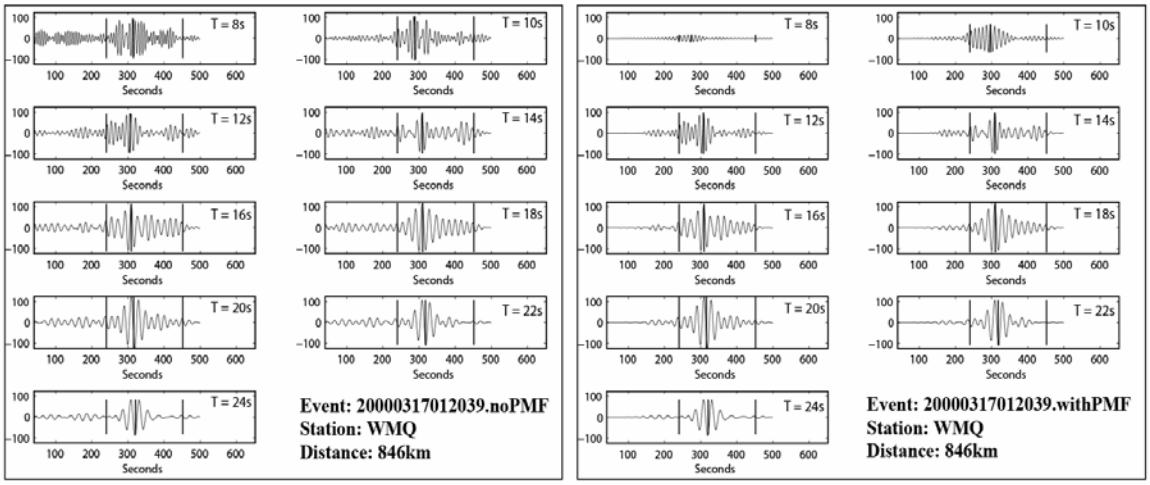

Figure 7. Data from the sample event shown in Figures 4-6. (Left) Narrow-band Butterworth "comb" filters applied to data that have not been PMF'd. (Right) The same filters applied to data that have undergone PMF'ing. Since this event is fairly large and close to the station, with a good signal-to-noise ratio, the PMF doesn't make much difference.

Our M_s program automatically chooses the period of maximum amplitude, but if the signal-to-noise ratio is low, it asks the analyst to check the pick. The analyst can then approve the program's pick, choose a different period, or eliminate the station from the analysis. One of the reasons that this analysis is done in the time domain is that it allows the analyst to visually confirm that the chosen amplitude corresponds to the fundamental mode, and not to possible multipathing or leakage that can contribute to the PMF results, or noise that obscures the Rayleigh phase. Once the period of maximum amplitude is chosen, an M_s is calculated. A mean and standard deviation of the M_s for each station is then calculated. Figure 8 shows the final output of the program for the sample event, for both phase match filtered (right) and non-phase match filtered (left) data.

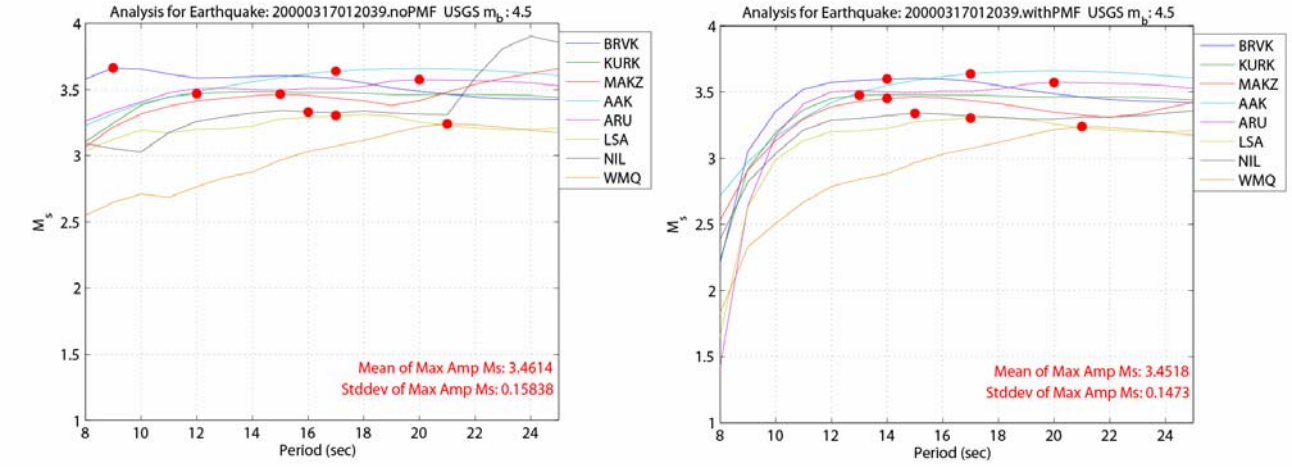

Figure 8. Final output of the M_s program for the sample event shown in Figures 4-7. (Left) The individual M_s estimates for the non-PMF'd data, as well as the mean M_s and standard deviation. (Right) The individual M_s estimates for the PMF'd data, as well as the mean M_s and standard deviation. Since this event is fairly large and close to the station, with good signal-to-noise ratio, the PMF doesn't make much difference in the final result. It did, however, reduce the variance and improve the M_s estimation at a few stations. The red dots are the maximum amplitude Ms for each station.

Pasyanos et al. (1999) show that use of the phase match filter generally results in a very slight lowering of the measured M_s, with the greatest change seen for $m_b < 5.0$. Preliminary results from this research show the same effect. In larger magnitude events, the use of the PMF has little or no effect on M_s: using 72 events with IDC $m_b \geq 3.4$, we found a mean M_s residual between the non-filtered data and the filtered data of 0.0363, with a sample standard deviation of the residual of 0.051. The standard deviation of the final M_s is generally close for the filtered and non-filtered data as well (Figure 9, right plot), although the difference between them is smaller for higher-magnitude events. When we extend our analysis to smaller events (IDC $m_b < 3.5$), we expect the PMFing to have a much greater effect on the standard deviation. One effect that was very noticeable in our preliminary study was that the use of the PMF filter often allows us to use more stations in the M_s analysis for a given event (Figure 9, left plot), by improving the signal-to-noise ratio for noisy stations which would otherwise have to be discarded from the analysis.

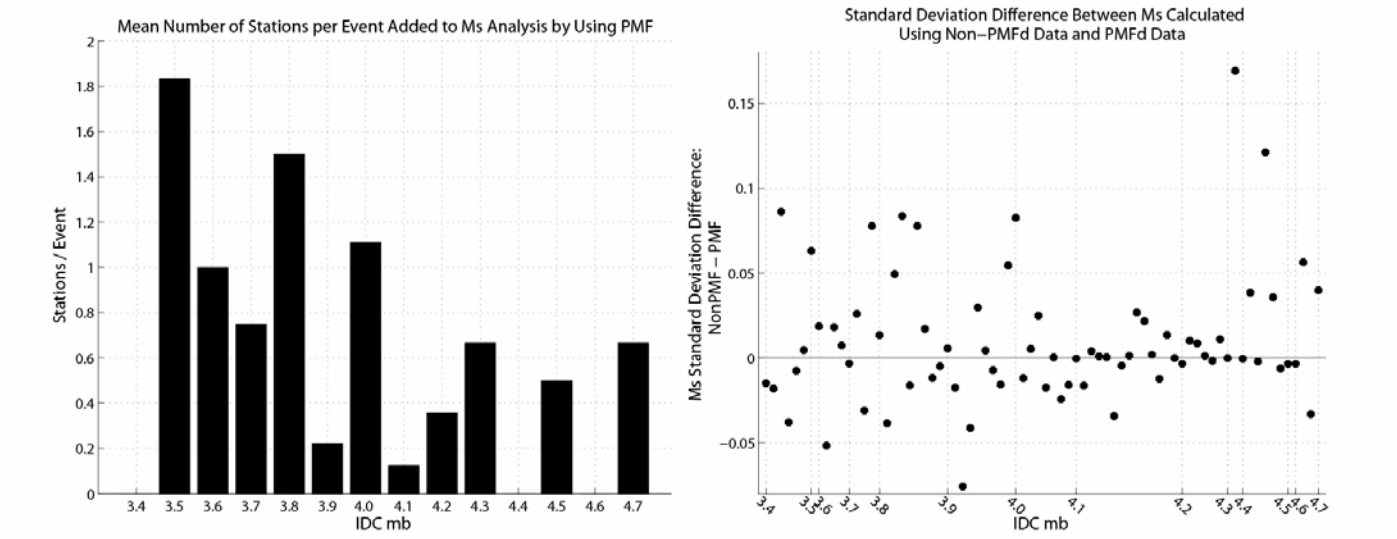

Figure 9. (Left) PMF'ing the data can improve the SNR at noisy stations, which often allows us to use more stations in the M_s analysis, particularly for smaller-magnitude events. To show this effect, we subtracted the number of stations used in the M_s analysis without PMF from the number of stations used with PMF for each event (for a total of 72 events), binned the events according to IDC m_b, and divided by the number of events in each bin. (Right) The difference in the M_s standard deviation between data that have not been PMF'd and data that have been PMF'd.

Figure 10 shows the M_s results for all 72 events analyzed thus far, with IDC $m_b \geq 3.4$, depth < 50km, and event-station distances from 200 to 4000 km. The solid diagonal line is the event screening equation $M_s = 1.25m_b - 2.2$ from Murphy et al. (1997). Note that all but two of the events fall above the discrimination line.

CONCLUSIONS AND FUTURE WORK

During the initial phases of this research project, we have extended the geographic coverage and lowered the periods of existing group velocity tomography maps in southern Asia. We have developed both a semi-automated Rayleigh wave detector and an automated phase match filtering routine which allow us to verify that Rayleigh phases are present and extract them from the waveforms. We have had success in the preliminary application of these new research products, along with the Russell (2005) surface wave formula, to a Eurasian dataset of events with $m_b < 5$.

In future phases of this research, we will calibrate the Russell (2005) and other magnitude formulas for regional distance applications. We will apply them, as part of our new methodology, to estimate M_s for earthquakes, quarry blasts, and explosions in Eurasia and southern Asia. We will also develop empirical and theoretical M_s threshold maps, based on the use of these calibrated, variable-period formulas and improved signal processing techniques. The new M_s thresholds will be compared with methods currently used in nuclear explosion monitoring to quantify any significant improvements obtained by using short-period surface waves.

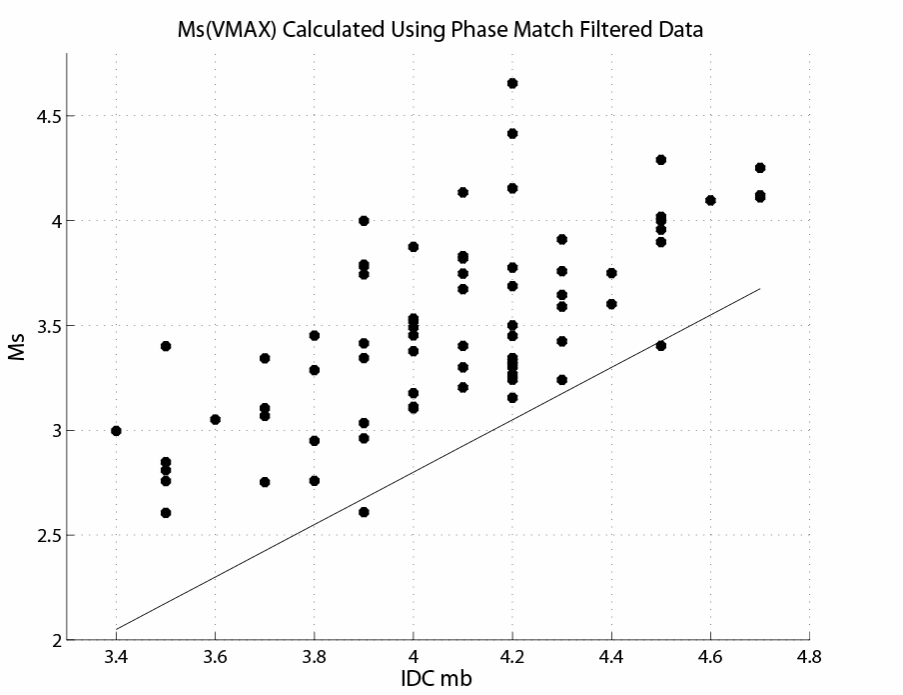

Figure 10. M_s results for all 72 events analyzed thus far, with IDC $m_b \geq 3.4$, depth < 50km, and event-station distances from 200 to 4000 km. The diagonal line is the event screening line from Murphy et al., 1997.

ACKNOWLEDGEMENTS

Thanks to Anastasia Stroujkova for insightful comments and ideas on improving the Rayleigh detector.

REFERENCES

Bonner, J. L., D. Russell, D. G. Harkrider, D. T. Reiter, and R. B. Herrmann (2005), Application of a time-domain, variable-period surface wave magnitude measurement procedure at regional and teleseismic distances – Part II: Application and M_s-m_b Performance, submitted to *Bull. Seism. Soc. Am.*

Chael, E. P. (1997), An Automated Rayleigh-Wave Detection Algorithm, *Bull. Seism. Soc. Am.* 87: 157–163.

Herrin, E.T. and T. Goforth (1977), Phase-match filtering: application to the study of Rayleigh Waves, *Bull. Seism. Soc. Am*. 67: 1259–1275.

Herrmann, R. B. (2004), *Computer programs in seismology*, St. Louis University.

Levshin, A., J. Stevens, M. Ritzwoller, and D. Adams (2002), Short-period (7s to 15s) group velocity measurements and maps in Central Asia, in *Proceedings of the 24th Seismic Research Review - Nuclear Explosion Monitoring: Innovation and Integration*, LA-UR-02-5048, Vol. 1, pp. 97–106.

Marshall, P.D. and P.W. Basham (1972), Discrimination between earthquakes and underground explosions Employing an Improved M_s Scale, *Geophys. J. R. Astr. Soc*. 29: 431–458.

Mitra, S. K. Priestley, V. K. Gaur, S. S. Rai, and J. Haines (in review), Variation in group velocity dispersion and seismic heterogeneity of the Indian Lithosphere, submitted to *Geophys. J. Int.*

Murphy, J. R., B. W. Barker, and M. E. Marshall (1997), Event screening at the IDC using the M_s/m_b discriminant, Maxwell Technologies Final Report, 23 p.

Pasyanos, M.E., W. R. Walter, S. R. Ford and S. E. Hazler (1999), Improving m_b:M_s discrimination using phase matched filters derived from regional group velocity tomography, in *Proceedings of the 21st Seismic Research Symposium - Technologies for Monitoring the Comprehensive Nuclear-Test-Ban Treaty*, LA-UR-99-4700, Vol. 2, 565–571.

Pasyanos, M., W. Walter, and M. Flanagan (2003), Geophysical models for nuclear explosion monitoring, in *Proceedings of the 25th Seismic Research Review - Nuclear Explosion Monitoring: Building the Knowledge Base*, LA-UR-03-6029, Vol. 1, 125–129.

Rezapour, M., and R.G. Pearce (1998), Bias in Surface-Wave Magnitude M_s Due to Inadequate Distance Correction, *Bull. Seism. Soc. Am*. 88: 43–61.

Russell, D.R. (2005), Development of a time-domain, variable-period surface wave magnitude measurement procedure for application at regional and teleseismic distances. Part I – Theory, submitted to *Bull. Seism. Soc. Am*.

Selby, N. D., (2001), Association of Rayleigh Waves using back azimuth measurements: application to test ban verification, *Bull. Seism. Soc. Am.* 91: 580-593.

Stevens, J. L. and K.L. McLaughlin (2001), Optimization of Surface Wave Identification and Measurement, in Monitoring the Comprehensive Nuclear Test Ban Treaty: Surface Waves, eds. Levshin, A. and M.H. Ritzwoller, *Pure Appl. Geophys*. 158: 1547–1582.

Taylor, S., X. Yang, W. Phillips, H. Patton, M. Maceira, H. Hartse, and G. Randall (2003), Regional event identification research in Eastern Asia, in *Proceedings of the 25th Seismic Research Review - Nuclear Explosion Monitoring: Building the Knowledge Base*, LA-UR-03-6029, Vol. 1, 476–485.

Tibuleac, I. M., J. Britton, D. B. Harris, T. Hauk, H. Hooper and J. L. Bonner (2004), Detection methods for mining explosions in Southern Asia, in *Proceedings of the 26th Seismic Research Review: Trends in Nuclear Explosion Monitoring*, LA-UR-04-5801, Vol. 1, 366–374.

Yacoub, N. K. (1983), Instantaneous amplitudes: A new method to measure seismic magnitude, *Bull. Seism. Soc. Am*. 73: 1345–1355.